ACS APPLIED MATERIALS & INTERFACES

Research Article

www.acsami.org

Single Ion Conducting, Polymerized Ionic Liquid Triblock Copolymer Films: High Capacitance Electrolyte Gates for n-type Transistors

Jae-Hong Choi,[†] Wei Xie,[‡] Yuanyan Gu,[†] C. Daniel Frisbie,*[,‡] and Timothy P. Lodge*[,†,‡]

[†]Department of Chemistry, University of Minnesota, 207 Pleasant Street SE, Minneapolis, Minnesota 55455, United States

[‡]Department of Chemical Engineering and Materials Science, University of Minnesota, 421 Washington Avenue SE, Minneapolis, Minnesota 55455, United States

Supporting Information

ABSTRACT: There has been impressive progress in the fabrication and characterization of p-type organic electrolyte-gated transistors (EGTs). Unfortunately, despite the importance of n-type organic transistors for complementary circuits, fewer investigations have focused on developing electrolytes as gate dielectrics for n-type organic semiconductors. Here, we present a novel single ion conductor, a polymerized ionic liquid (PIL) triblock copolymer (PS-PIL-PS) composed of styrene (PS) and 1-[(2-acryloyloxy)ethyl]-3-butylimidazolium bis(trifluoromethylsulfonyl)imide (PIL), that conducts only the TFSI anion. This triblock copolymer acts as a gate dielectric to allow low-voltage n-type organic EGT operation. Impedance characterization of PS-PIL-PS reveals that there are three polarization regions: (1) dipolar relaxation, (2) ion migration, and (3) electric double layer (EDL) formation. These polarization regions are controlled by film thickness, and rapid EDL formation can be obtained in thinner polyelectrolyte films. In particular, a 500 nm-thick polyelectrolyte film exhibits a large capacitance of ~1 μF/cm^2 at 10 kHz. Employing this single ion conducting PIL triblock copolymer as the gate insulator, we achieved low voltage operation (<1 V supply) of poly{[*N*,*N*′-bis(2-octyldodecyl)-naphthalene-1,4,5,8-bis(dicarboximide)-2,6-diyl]-*alt*-5,5′-(2,2′-bithiophene)} (P(NDI2OD-T2)) n-type organic EGTs (electron mobility of ~0.008 cm^2/(V·s) and ON/OFF current ratio of ~2 × 10^3) by preventing electrochemical doping. Furthermore, the recognition that the performance of n-type organic EGTs is diminished by 3D electrochemical doping suggests that it may be necessary to have a unipolar electrolyte to gate n-type organic semiconductors. Finally, we highlight that the use of PIL block copolymer electrolytes as gate insulators opens unique opportunities to explore the role of ion penetration in n-type organic EGTs by tuning the extent of electrochemical doping.

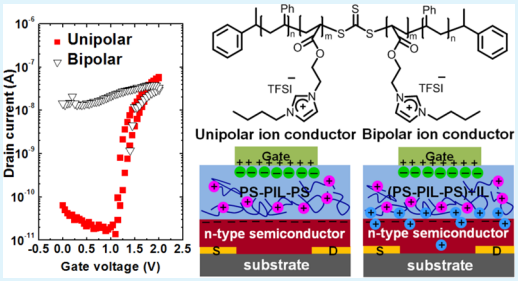

KEYWORDS: *polymerized ionic liquid, polyelectrolyte, single ion conductor, organic semiconductor, thin-film transistor*

INTRODUCTION

The field of printed organic electronics has attracted substantial interest as the demand for conformal, lightweight electronics has increased. A key component in many potential organic electronic devices, including displays, chemical sensors, and radio frequency identification (RFID) tags, is the thin film transistor (TFT).[1−9] In the development of organic TFTs, an important challenge for practical devices is reduction of the operating voltage. An attractive direction is to employ an electrolyte as the gate insulator, because it provides extremely high capacitance (1−10 μF/cm^2). Several groups have reported electrolyte-gated thin film transistors based on graphene,[10−12] organic,[13−20] and inorganic semiconductors.[21−26]

There are two operative mechanisms for electrolyte-gated transistors (EGTs) in which an ionically conducting and electronically insulating electrolyte serves as the gate insulator.[4,27] In the case of ion-impermeable inorganic and organic single crystal semiconductors, ions in the electrolytes migrate and accumulate at the gate/electrolyte and electrolyte/semiconductor interfaces upon application of a gate voltage. The accumulated ions and induced counter-charges form two-dimensional (2D) electric double layers (EDLs) at each interface. The resulting large local electric field at the electrolyte/semiconductor interface induces high charge density accumulation in the semiconductor channel, yielding a significant reduction in the operating voltage and a substantial increase in the source-drain current. EGTs with impermeable semiconductors are also referred to as electric double layer transistors (EDLTs).[28,29] On the other hand, for transistors with ion-permeable semiconductors such as conjugated polymers, electrolyte ions can diffuse into the film upon application of a gate voltage. A "clean" EDL may be formed only at the gate/electrolyte interface. In this case, the gating mechanism is electrochemical doping and dedoping of the semiconductor channel upon application and removal of a gate voltage, respectively. EGTs operating in this mode are also referred to as electrochemical transistors (ECTs). Although it is expected that the structure of an organic semiconductor film

Received: January 16, 2015
Accepted: March 17, 2015
Published: March 30, 2015

DOI: 10.1021/acsami.5b00495
ACS Appl. Mater. Interfaces 2015, 7, 7294−7302

will be disrupted by electrochemical doping, the formation of a 3D channel by bulk ion doping can result in enormous drive currents, which may be favorable for specific applications. Despite successful demonstration of both types of EGTs, understanding of the effects of electrochemical doping on device performance in EGTs remains incomplete.

Furthermore, to realize organic integrated circuits with low power consumption for portable devices, one of the most important challenges is the design of complementary EGT circuits including both organic p-type and n-type semiconductors. There has been enormous progress in demonstrating high-performance organic p-type EGTs,[15−17,30−34] but organic n-type EGTs remain relatively unexplored.[35−39] Panzer et al.[35] reported an n-type polycrystalline organic semiconductor EGT using a poly(ethylene oxide) (PEO)/lithium perchlorate polymer electrolyte. Ono et al.[36] and Uemura et al.[37] demonstrated low-voltage operation of n-type organic single crystal EGTs using ionic liquids as gate insulators. More recently, in work employing unipolar polyelectrolytes, where one of the ions (either cation or anion) is incorporated into a polymer chain and therefore is immobilized while the other ion is mobile, Malti et al.[38] and Herlogsson et al.[39] reported air-stable, low voltage n-type organic EGTs and complementary circuits, respectively. The fundamental question then arises as to whether it is necessary to have unipolar electrolyte to gate n-type organic semiconductors, instead of a bipolar electrolyte.

Polymerized ionic liquids (PILs) are a new class of unipolar polyelectrolytes or single ion conductors, where ionic liquid moieties are covalently attached to the polymer backbone or side chains, while the counterions are mobile. Because ionic liquid functionalities are directly incorporated into the macromolecular structures, these systems possess both the functional properties of ionic liquids (e.g., high ionic conductivity, wide electrochemical window, negligible vapor pressure, nonflammability, and good chemical and thermal stability) and the flexibility and mechanical strength of macromolecules. Therefore, PILs have been explored as promising candidates for polymer electrolytes in electrochemical applications such as batteries, fuel cells, supercapacitors, gas separation membranes, and solar cells.[40−44] The properties of PILs are strongly related to both the ionic liquid and the polymer structures, so they provide great design flexibility. The principal figures of merit describing the improvement of polymer electrolytes are high ionic conductivity and elastic modulus. Much effort has been directed at lowering the glass transition temperature (T_g) of the PIL to enhance ionic conductivity, but these materials with lower T_g inevitably sacrifice mechanical strength.[45,46] Thus, block copolymers combining an ion-conducting PIL with mechanically robust microdomains may be advantageous materials as compared to ion gels[15,47] and PIL homopolymers[48] in the design of polymer electrolytes. Additionally, because electrochemical doping can be controlled by gating with a unipolar polyelectrolyte, a PIL polyelectrolyte should enrich the spectrum of workable EGTs. We are not aware of a previous report on EGTs employing PILs as gate insulators.

Here, we introduce a novel solid polymer electrolyte based on a PIL as a gate insulator for EGTs. We describe the fabrication and characterization of n-type organic EGTs with a PIL triblock copolymer (PS-PIL-PS) composed of styrene (S) and 1-[(2-acryloyloxy)ethyl]-3-butylimidazolium bis(trifluoromethylsulfonyl)imide (PIL). Unlike other electrolytes such as ionic liquids and ion gels, this PS-PIL-PS polyelectrolyte is a single ion conductor because one of the ionic moieties is covalently linked to the backbone. The dual purpose of this study is (a) to enrich the fundamental understanding of impedance behavior in a unipolar ion conductor, and (b) to demonstrate the ability to use a unipolar ion conductor as the gate insulator in n-type organic EGTs. We show that the impedance behavior of PS-PIL-PS polyelectrolytes exhibits three polarization regions: (1) dipolar relaxation, (2) ion migration, and (3) EDL formation. These polarization mechanisms shift toward higher frequencies as film thickness decreases. Importantly, a 500 nm-thick polyelectrolyte film exhibits a large capacitance of ~1 μF/cm^2 at 10 kHz, which is a key parameter for low-voltage EGT operation. Employing this unipolar ion conductor as a gate dielectric prevents electrochemical doping and allows us to achieve n-type organic EGTs. This work also highlights that the performance of n-type organic EGTs is limited by electrochemical doping of the semiconductor by mobile cations from the electrolyte.

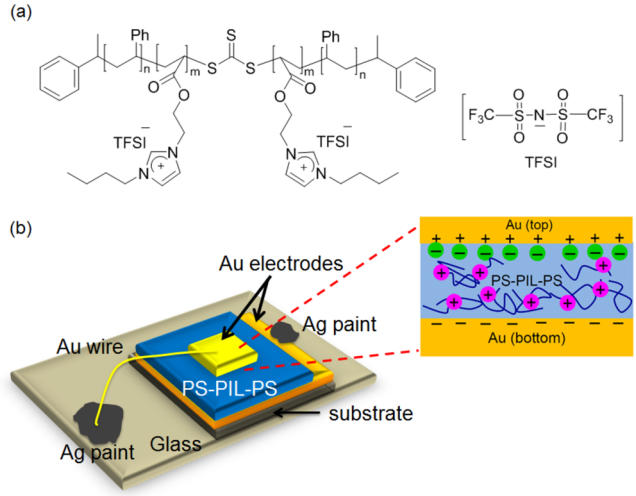

Figure 1. (a) Chemical structure of ABA triblock copolymer with a polymerized ionic liquid midblock, poly(styrene-*b*-1-[(2-acryloyloxy)-ethyl]-3-butylimidazolium bis(trifluoromethyl sulfonyl)imide-*b*-styrene) (PS-PIL-PS). (b) Schematic shows the Au/PS-PIL-PS/Au capacitor used to measure impedance properties (not to scale). Cations are covalently tethered to the polymer backbone, while anions (TFSI) are mobile. The Au top electrode was fabricated by thermal evaporation with a shadow mask.

RESULTS AND DISCUSSION

Impedance Behavior of PIL Electrolyte Dielectrics. Figure 1a shows the chemical structure of the PS-PIL-PS triblock copolymer with an acrylate-based midblock.[42] In this PIL block copolymer, the cation is covalently anchored into the polymer side chains so that it is immobilized, while the counterion, TFSI anion, is free to move. Figure 1b displays the metal−polyelectrolyte (insulator)−metal (MIM) capacitor used to measure impedance properties of the PS-PIL-PS polyelectrolyte. This MIM sandwich structure was fabricated by evaporating a gold top electrode onto a spin coated polyelectrolyte film as described in the Experimental Section. Application of a voltage across the MIM capacitor causes the mobile TFSI anions to move, and EDLs are formed at the electrolyte/electrode interfaces as depicted. As compared to bipolar ion conductors such as ion gels and ionic liquids, the

DOI: 10.1021/acsami.5b00495
ACS Appl. Mater. Interfaces 2015, 7, 7294−7302

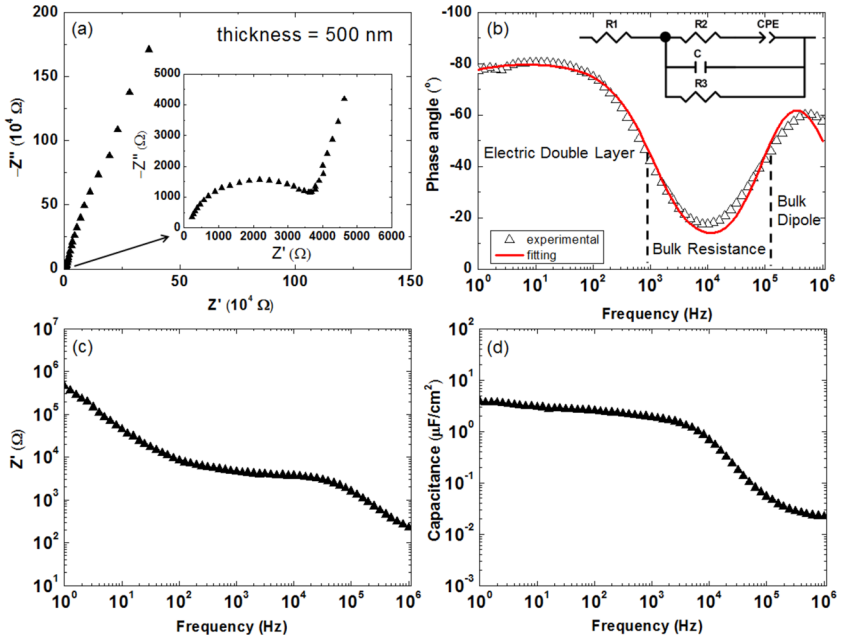

Figure 2. (a) Nyquist plots, (b) phase angle versus frequency, (c) Z' versus frequency, and (d) specific capacitance of a 500 nm-thick PS-PIL-PS electrolyte film. The inset in (a) shows the expanded Nyquist plot in the high frequency region. In (b), the symbols indicate experimental data, while the solid lines represent the fit of the data to the impedance model (equivalent circuit) in inset. In the impedance model, C, $R1$, $R2$, and $R3$ correspond to dipolar polarization at high frequencies, contact resistance, bulk resistance of electrolyte, and resistance from leakage current, respectively. The impedance of the constant phase element (CPE) is defined as $Z_{CPE} = Q_n^{-1}(j\omega)^{-n}$, where Q_n is a constant, j is the imaginary number, ω is the angular frequency ($\omega = 2\pi f$), and n is a constant in the range $0 \leq n \leq 1$.

Table 1. Fitting Parameters from the Circuit Components in the Impedance Model of PS-PIL-PS Capacitors with Various Thicknesses

thickness (mm)	$R1$ (Ω)	n	Q_n	$R2$ (kΩ)	C (nF)	$R3$ (MΩ)
1.5×10^{-4}	7.0×10^{1}	0.78	2.6×10^{-7}	1.02×10^{0}	1.7	0.0037
2.0×10^{-4}	8.0×10^{1}	0.86	1.4×10^{-7}	1.15×10^{0}	1.3	0.016
5.0×10^{-4}	2.3×10^{2}	0.90	9.3×10^{-8}	3.45×10^{0}	0.50	38
3.0×10^{-3}	1.3×10^{3}	0.86	1.1×10^{-7}	1.53×10^{1}	0.10	6.0
1.0×10^{-2}	3.3×10^{3}	0.87	9.1×10^{-8}	5.06×10^{1}	0.040	7.9
4.3×10^{-2}	1.0×10^{4}	0.82	1.3×10^{-7}	1.30×10^{2}	0.020	8.4
2.0×10^{0}	N/A	0.68	1.8×10^{-7}	1.02×10^{3}	0.0050	N/A

thickness of the EDL established by the mobile TFSI anions is expected to be smaller than that of the EDL formed by the larger polycations, and therefore the capacitance of the two EDLs will not be the same. Because the capacitance of an EDL is inversely proportional to its thickness,[4,49] we anticipate that the capacitance of the EDL formed by smaller TFSI anions will be significantly higher.

Figure 2 displays the results of impedance spectroscopy experiments on 500 nm-thick PS-PIL-PS block copolymer films sandwiched between two Au electrodes. The Nyquist plot (Z'' versus Z') in Figure 2a shows a semicircle at higher frequencies (10^6–10^4 Hz, see the inset) and a tilted straight line at lower frequencies (10^4–1 Hz), which corresponds to the typical behavior of electrolytes in contact with solid electrodes.[50] Figure 2b shows the phase angle as a function of frequency. The polarization of typical polyelectrolytes exhibits both capacitive behavior (phase angles lower than −45°) and resistive behavior (phase angles greater than −45°).[13] The 500 nm-thick polyelectrolyte film shows two transitions between capacitive and resistive character at ∼120 kHz and ∼850 Hz. The capacitive behavior at high frequencies (f > 120 kHz) is attributed to the dipolar relaxation between cations and anions of the polyelectrolyte. The resistive character at intermediate frequency region (850 Hz < f < 120 kHz) results from migration of mobile anions. The capacitive behavior at low frequencies (f < 850 Hz) is related to the formation of EDLs at the polyelectrolyte/metal electrode interfaces. These three frequency-dependent polarization regions have been also observed in other polyelectrolytes.[13]

On the basis of the Nyquist and phase angle versus frequency plots, the experimental impedance results are modeled with an equivalent circuit, shown as an inset to Figure 2b. The equivalent circuit contains a capacitor (C) corresponding to the polarization of the dipoles within the polyelectrolyte and a resistor ($R2$) in parallel reflecting the bulk resistance from ion migration at high frequencies, which gives rise to a semicircle in a Nyquist plot. At low frequencies, the equivalent circuit is composed of the bulk resistor ($R2$) in series with a capacitor corresponding to the establishment of EDLs at interfaces, which results in a vertical line in a Nyquist plot. However, it is known that the capacitance dispersion related to the surface roughness of metals in contact with electrolytes leads to deviation from ideal capacitor behavior, so the vertical line becomes tilted as seen in the Nyquist plot in Figure 2a.[49−52] To

DOI: 10.1021/acsami.5b00495
ACS Appl. Mater. Interfaces 2015, 7, 7294−7302

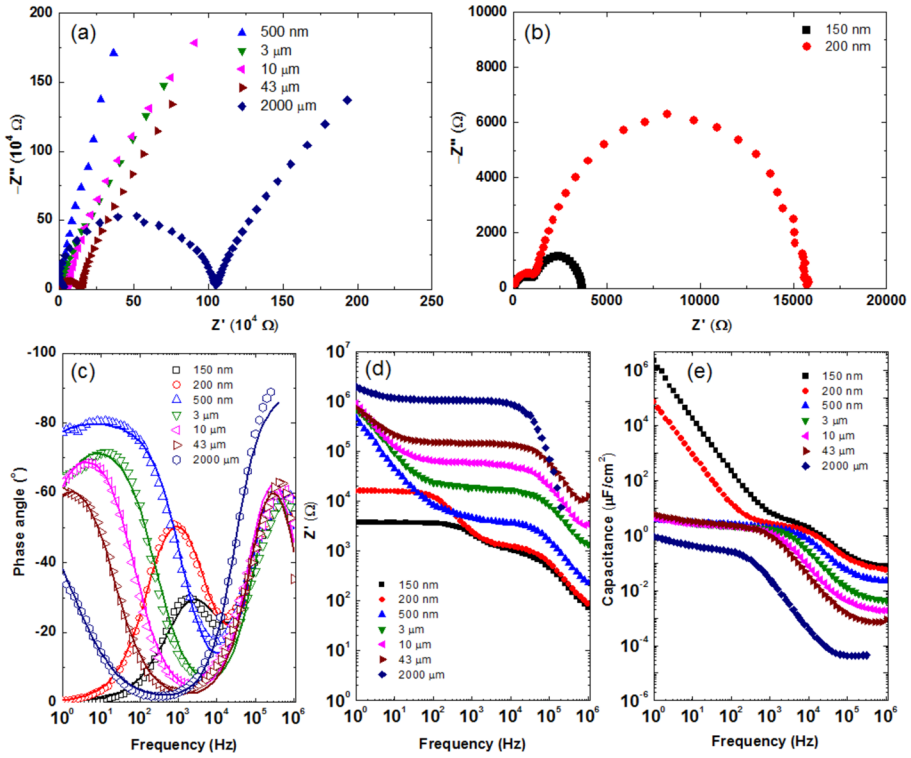

Figure 3. Nyquist plots of PS-PIL-PS electrolyte-based capacitors with various thicknesses of (a) 500 nm to 2000 μm and (b) 150 and 200 nm. (c) Phase angle versus frequency, (d) Z' versus frequency, and (e) specific capacitance for PS-PIL-PS films with various thicknesses. Solid lines in (c) are a fit to an equivalent circuit model. The phase angle data in panel c suggest that the thinnest films have electrical shorts and hence high leakage currents.

account for the deviation in impedance behavior of the electrolytes caused by the inhomogeneous interfaces, we employ a constant phase element (CPE) in the equivalent circuit instead of an ideal capacitor. The impedance of the CPE is expressed as[13,49,51]

$$Z_{\mathrm{CPE}} = Q_n^{-1}(j\omega)^{-n} \quad (1)$$

where Q_n is a constant, j is the imaginary number, ω is the angular frequency ($\omega = 2\pi f$), and n is a constant in the range $0 \leq n \leq 1$. The phase angle is determined by $\theta_{\mathrm{CPE}}(n) = -90n°$: $n = 1$ represents an ideal capacitor with capacitance $C = Q_n$, and $n = 0$ corresponds to an ideal resistor with resistance $R = Q_n^{-1}$. In addition, two resistors, $R1$ (representing the nonideal contact resistance) and $R3$ (corresponding to the resistance from leakage current of the material), are added in series and in parallel to the equivalent circuit, respectively. The proposed equivalent circuit model shown in the inset of Figure 2b describes the experimental impedance results for the 500 nm-thick PS-PIL-PS polyelectrolyte film well; the fitting parameters are summarized in Table 1. The capacitance (C) from dipolar relaxation at high frequencies is about 0.5 nF, which is much smaller than the capacitance from electrical double layers. The value of $R1$ (~230 Ω), corresponding to the nonideal contact resistance, is significantly smaller than the value of $R3$ (~38 MΩ) related to the resistance from leakage current of the electrolyte. The value of n is ~0.9, which implies that the CPE is related to the capacitance from the formation of electrical double layers.

Figure 2c displays the measured Z' versus frequency. The nearly frequency-independent behavior at intermediate frequencies reflects the bulk resistance of ion migration, consistent with the interpretation of the phase angle plot described above. The value (~3400 Ω) in the plateau is comparable to the $R2$ value obtained by fitting. The calculated ionic conductivity of the 500 nm-thick PS-PIL-PS polyelectrolyte film is therefore ~ 1×10^{-3} mS/cm at room temperature. Figure 2d shows the calculated effective specific capacitance as a function of frequency. The capacitance values increase with decreasing frequency and are greater than ~1 μF/cm^2 at frequencies below 10 kHz. The large capacitance of the PS-PIL-PS polyelectrolyte, in the range of 1−4 μF/cm^2, is attributable to the establishment of the EDLs at the electrode/polyelectrolyte interfaces. Also, an equivalent circuit with a constant phase element provides a frequency-independent effective capacitance from R and the fitting parameters:[49,51]

$$C = R^{((1/n)-1)}Q_n^{1/n} \quad (2)$$

The extracted frequency-independent capacitance is ~2 μF/cm^2, which compares favorably to other ionic liquid incorporated electrolytes.[49,53]

The impedance properties of PS-PIL-PS polyelectrolyte films were also investigated systematically as a function of film thickness. Figure 3a−e shows Nyquist plots, phase angle versus frequency, Z' versus frequency, and specific capacitance versus frequency for PS-PIL-PS polyelectrolyte films ranging in thickness from 150 nm to 2000 μm. As illustrated in Figure 3a, the Nyquist plots show a semicircle at high frequencies and a tilted straight line at low frequencies for polyelectrolyte films with a thickness ranging from 500 nm to 2000 μm, which is consistent with the previous observation. However, the Nyquist plots for 150 nm- and 200 nm-thick films exhibit two semicircles over the measured frequency range (1−10^6 Hz),

DOI: 10.1021/acsami.5b00495
ACS Appl. Mater. Interfaces 2015, 7, 7294−7302

as seen in Figure 3b. This is clearly in contrast to the polarization behavior at low frequencies observed in Figure 3a.

The experimental impedance results were modeled using the same equivalent circuit. Figure 3c displays phase angle versus frequency of PS-PIL-PS polyelectrolytes and the model fits from the equivalent circuit at various film thicknesses. Experimental results for all samples are in good agreement with the proposed circuit model. For films with a thickness ranging from 500 nm to 43 μm, three polarization regions of polyelectrolytes were observed over the measured frequency range as discussed above: dipolar relaxation (bulk capacitance), ion migration (bulk resistance), and the formation of EDLs. The transition from ion migration to EDL formation occurs at 950 Hz for the 500 nm-thick film, whereas the transition happens at 12 Hz for the 43 μm-thick sample. This ~80-fold difference in the transition frequency is comparable to the ratio of the film thicknesses.

The phase angle plot of the 2000 μm-thick film (bulk sample) indicates capacitive behavior due to dipolar relaxation and resistive behavior due to ion migration, while the EDL formation from mobile TFSI anions is impeded in the measured frequency range (down to 1 Hz) due to the significantly larger film thickness (2000 μm) and slower ion mobility of PILs. The contributions of both the resistor related to nonideal contacts ($R1$) and the resistor associated with leakage current ($R3$) are negligible because $R1$ is small relative to the other resistance in series, and the large $R3$ has little effect because it is combined in parallel.

In contrast, both the 150 and the 200 nm-thick samples show resistive behavior at frequencies below 1000 Hz, rather than a capacitive behavior related to EDL formation. As seen in the fitting parameters (Table 1), the values of the resistance related to the leakage current ($R3$) are much lower than those of other samples, and dominate the impedance behavior at low frequencies. Because the glass transition temperature of the PIL midblock (84% in weight fraction) is −9 °C, we speculate that the formation of small pinholes in such a thin film during the thermal evaporation of the metal electrodes causes a significant leakage current.

Figure 3d shows Z' versus frequency at various thicknesses. The frequency-independent real impedance values (the plateau in the Z' versus frequency plot, corresponding to the resistance of ion migration for PS-PIL-PS polyelectrolytes) decrease with decreasing film thickness, which is consistent with previous observations in ion gels.[50] Figure 3e shows the calculated specific capacitance as a function of frequency. For polyelectrolyte films with a thickness ranging from 500 nm to 43 μm, the capacitances in the range of 4−6 μF/cm^2 are obtained due to the formation of the EDLs at the electrode/polyelectrolyte interfaces, which are independent of film thickness. As the film thickness decreases, the frequency corresponding to ~1 μF/cm^2 shifts toward higher frequencies, which indicates that EDL formation is more rapid in thinner polyelectrolyte films. The lower capacitance value (0.2−0.9 μF/cm^2) at low frequencies for the 2000 μm-thick film is due to the impeded formation of the EDL by mobile TFSI anions as mentioned above. We expect that the capacitance in the range of 0.2−0.9 μF/cm^2 originates from the thick EDL formation by immobile polycations. It is worth noting that, although the PS-PIL-PS unipolar polyelectrolyte has a relatively lower ionic conductivity than other bipolar ion conductors such as neat ionic liquids and ion gels, a capacitance above 1 μF/cm^2 can still be obtained at 10 kHz by employing PS-PIL-PS films with a thickness of 500 nm. This suggests that this hydrophobic, unipolar PS-PIL-PS polyelectrolyte can be applicable to thin film transistors as a gate insulator.

We also investigated the effect of temperature on ionic conductivity and capacitance for the PS-PIL-PS polyelectrolyte (see Supporting Information Figure S1). The ionic conductivity for a 2000 μm-thick film increased with increasing temperature, which is attributed to the enhanced segmental relaxation of PILs at elevated temperature.[41,46] The ionic conductivity is ~4 × 10^{-3} mS/cm at 30 °C and reaches ~0.7 mS/cm at 95 °C. In addition, the capacitance of the polyelectrolyte films increases with increasing temperature. Although the physical origins of this behavior are still under investigation, it has been reported that the temperature-dependent capacitance can be attributed to the increased free ion concentration at high temperature.[50] Note that an increased ionic conductivity with increasing temperature leads to rapid EDL formation. Therefore, the capacitance value for a PS-PIL-PS polyelectrolyte at 95 °C is greater than ~0.5 μF/cm^2 at 100 kHz. Thus, we anticipate that the dynamic characteristics of the transistors gated with this PS-PIL-PS polyelectrolyte dielectric will warrant improvement, because this PIL polyelectrolyte has lower room temperature ionic conductivity than bipolar ion gels. Nevertheless, PIL electrolytes with high ionic conductivity could be very promising candidates as gate insulators for faster switching devices.

Unipolar Ion Conducting Electrolyte Dielectrics for n-type EGTs. We tested the unipolar ion conducting PS-PIL-PS polyelectrolyte as a gate insulator in electrolyte gated TFTs. Particularly, because this PIL electrolyte is a polycationic electrolyte where only the anion is mobile, we fabricated top-gated n-type organic TFTs to prevent 3D electrochemical doping, as depicted in Figure 4a (left). Application of a positive gate bias causes mobile TFSI anions to migrate toward the gate, leaving bulky polycations at the semiconductor/polyelectrolyte interface. We anticipate that these bulky cations cannot penetrate into semiconductor layer, so they establish a 2D EDL. For an n-type organic semiconductor, we selected a commercially available and solution-processable poly{[*N*,*N*′-bis(2-octyldodecyl)-naphthalene-1,4,5,8-bis(dicarboximide)-2,6-diyl]-*alt*-5,5′-(2,2′-bithiophene)} (P(NDI2OD-T2)) n-type conjugated polymer, Figure 4a (right).[54] Figures 4b and c shows the quasi-static transfer and output characteristics of n-type P(NDI2OD-T2) EGTs (W/L = 1000 μm/10 μm) where thermally evaporated aluminum (t = 100 nm) and a 500 nm-thick PS-PIL-PS film were used for the gate electrode and the gate insulator, respectively. The transfer curve (drain current versus gate voltage) in Figure 4b was measured by sweeping V_G from −1 to 1 V and back to −1 V at a sweep rate of 50 mV/s. The n-type transistor displayed an ON/OFF current ratio of ~2 × 10^3. The current hysteresis between the forward and reverse traces can be attributed to the relatively lower ionic conductivity of the PS-PIL-PS polyelectrolyte. The measured specific capacitance is ~1 μF/cm^2, which is obtained from displacement current measurements. This high capacitance leads to the operation of n-type P(NDI2OD-T2) EGTs at low voltages. The electron mobility in the saturation regime was calculated from the following equation:

$$I_D = \frac{W}{2L} C\mu (V_G - V_{th})^2 \quad (3)$$

where C is the capacitance of the gate insulator, W is the channel width, L is the channel length, V_{th} is the threshold

DOI: 10.1021/acsami.5b00495
ACS Appl. Mater. Interfaces 2015, 7, 7294−7302

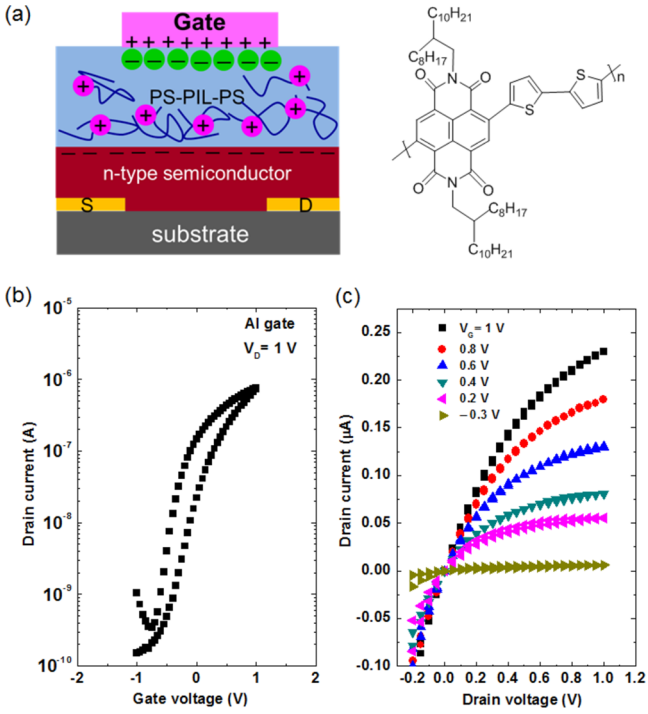

Figure 4. (a) A schematic cross section showing the polarization in a PS-PIL-PS electrolyte gated transistor based on an n-type semiconductor when applying a positive gate voltage (left). Chemical structure of the n-type semiconductor (P(NDI2OD-T2)) used in the device (right). (b) Transfer and (c) output characteristics of an n-type transistor with PS-PIL-PS polyelectrolyte gate dielectric. An aluminum gate electrode was vacuum-deposited through a shadow mask. The channel length and width are 10 and 1000 μm, respectively. The gate voltage was swept at a rate of 50 mV/s.

voltage, and μ is the field-effect mobility. The V_{th} obtained from the plot of $I_D^{1/2}$ versus V_G is −0.4 V, and the saturation charge carrier mobility is ∼0.008 cm^2/(V·s). The extracted electron mobility is comparable to previously reported values for other n-type P(NDI2OD-T2) EGTs.[38,39] The output curves (drain current versus drain voltage) at six different gate voltages (V_G) exhibited linear and saturation regimes with increasing V_G, as seen in Figure 4c. These results demonstrate that the unipolar polycationic PS-PIL-PS polyelectrolyte is a promising gate insulator for n-type organic EGTs.

Another important observation is that the surface of the PS-PIL-PS electrolyte is amenable to subsequent materials deposition, so that we are able to thermally evaporate metal electrodes directly onto the polyelectrolyte, which has typically been difficult for ion gels, for example. Also, the hydrophobic character enables various processes such as transferring or aerosol jet printing of hydrophilic PEDOT:PSS electrodes on the surface. We utilized this facile processability to investigate the effect of the work function of the gate material on the threshold voltage (V_{th}) in n-type organic EGTs (see Supporting Information Figure S2). We fabricated top-gated n-type P(NDI2OD-T2) EGTs with thermally evaporated aluminum, silver, gold, and aerosol jet printed PEDOT:PSS as gate electrodes. By changing gate materials from low work function Al to high work function PEDOT:PSS, we were able to tune the threshold voltage in the linear regime from 0 to 1 V in n-type organic EGTs. As seen in simplified energy band diagrams (Supporting Information Figure S2c), the Al gate electrode in n-type organic EFTs reduces the flatband voltage for electron accumulation as compared to the Au gate electrode, which results in a lower threshold voltage. The tunability of V_{th} by changing gate materials in n-type organic EGTs is consistent with previous observations in p-type organic EGTs,[55] and should provide new avenues to design organic integrated circuits. It is also expected that the use of a hydrophobic PIL block copolymer polyelectrolyte is beneficial to the stability of EGTs under humid conditions, as compared to other more hydrophilic polyelectrolytes.[39]

We also demonstrated p-type organic poly(3-hexylthiophene) (P3HT) EGTs using the same PS-PIL-PS polyelectrolyte gate insulator (see Supporting Information Figure S3). In this case, the application of a negative gate bias leads to the migration of mobile TFSI anions toward the polyelectrolyte/semiconductor interface, and TFSI anions can diffuse into the P3HT semiconductor film. Therefore, the operation mechanism of the device is affected by electrochemical doping and dedoping of the semiconductor channel. Both the transfer and the output characteristics of the devices exhibited good linear and saturation behavior at low and high drain voltages, respectively. As a consequence of the electrochemical doping and dedoping processes of TFSI anions with lower ion mobility in PILs, the transistors displayed a relatively large current hysteresis, which is dependent on the sweep rate. The measured capacitance determined from displacement current measurements in p-type P3HT EGTs is ∼10 μF/cm^2. The order of magnitude larger capacitance in P3HT as compared to P(NDI2OD-T2) EGTs is due to the 3D electrochemical doping in the semiconductor channel. The average hole mobility in the saturation regime was ∼0.07 cm^2/(V·s), and the devices showed an ON/OFF current ratio of ∼5 × 10^4.

Few successful demonstrations of n-type organic EGTs using a unipolar polycationic electrolyte as a gate insulator have been reported,[38,39] and the effect of electrochemical doping on the performance of n-type organic EGTs has not been examined. To address this point, the extent of electrochemical doping of mobile ions was controlled by adding different amounts of ionic liquid, [EMI][TFSI], to the PS-PIL-PS polyelectrolyte. The chemical structure of [EMI][TFSI] ionic liquid is illustrated in Figure 5a. As sketched in Figure 5b, in a unipolar polycationic electrolyte, bulky polycations cannot diffuse into the semiconductor layer, so a 2D electric double layer is created at the electrolyte/semiconductor interface. On the other hand, in bipolar ion conductors with [EMI][TFSI] ionic liquid, both immobilized polycations and mobile cations accumulate at the polyelectrolyte/semiconductor interface, and some mobile cations can penetrate the polymer semiconductor such that 3D channel is formed by the electrochemical doping.[16] Figures 5c and d shows the quasi-static transfer curves and gate current versus gate voltage for n-type organic P(NDI2OD-T2) EGTs with neat PS-PIL-PS and IL-doped PS-PIL-PS polyelectrolyte gate dielectrics. The transfer characteristic was obtained by sweeping V_G from 0 to 2 V at a sweep rate of 50 mV/s with a drain voltage (V_D) of 1 V. For the EGT with a neat PS-PIL-PS gate insulator, the transistor can operate at supply voltages below 2 V and exhibited an ON/OFF current ratio of ∼4 × 10^3 with a small current hysteresis. The gate leakage current was less than 2 nA and is much smaller than the channel current. Upon addition of 10 wt % [EMI][TFSI], the ON drain current of the transistor was reduced by an order of magnitude, while the OFF current was increased, such that the device exhibited a poor ON/OFF ratio. The transistor exhibited a small gate leakage current (<2 nA), and the difference between the

DOI: 10.1021/acsami.5b00495
ACS Appl. Mater. Interfaces 2015, 7, 7294−7302

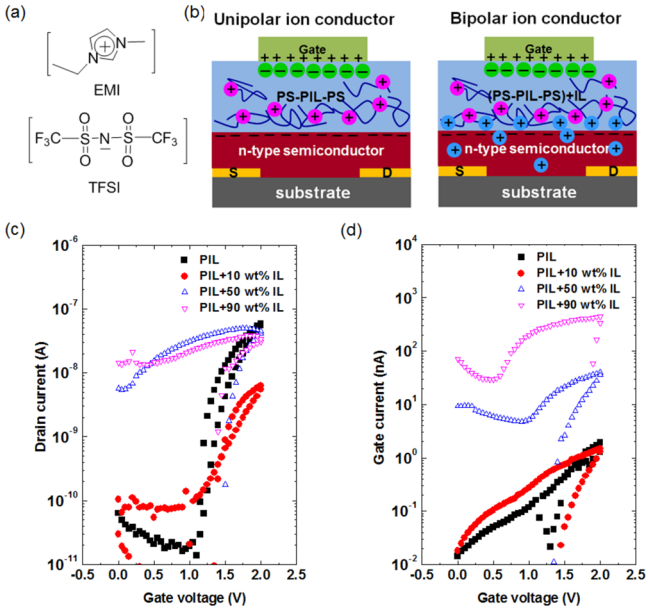

Figure 5. (a) Chemical structure of the ionic liquid, [EMI][TFSI]. (b) A schematic cross section showing the polarization in unipolar (neat PS-PIL-PS) and bipolar (IL-doped PS-PIL-PS) electrolyte gated transistors based on n-type semiconductors under positive gate voltage. (c) Transfer characteristics and (d) gate current–gate voltage of n-type transistors with neat PS-PIL-PS and IL ([EMI][TFSI])-doped PS-PIL-PS polyelectrolyte gate dielectrics. The channel length and width are 10 and 1000 μm, respectively. The gate voltage was swept at a rate of 50 mV/s. The PEDOT:PSS gate electrode was deposited by aerosol jet printing.

reduced channel current and gate leakage current became small. When the fraction of ionic liquid was increased further (to 50 and 90 wt %), the transistors no longer operated. The device performance was degraded by the large gate leakage current. These results indicate that the electrochemical doping of mobile cations into the semiconductor layer causes a gate leakage current, which deteriorates the performance of n-type organic EGTs. It has been reported that the large gate leakage current can be attributed to a redox reaction between the penetrating cations and organic molecules,[18,56] and the electrochemical doping is irreversible due to the partial trapping of cations in the semiconductor layer.[56]

To investigate the effect of the dopant ion type on the device performance in n-type organic EGTs, another IL [P14][TFSI] having a pyrrolidinium-type cation was doped into the neat PS-PIL-PS polyelectrolyte (see Supporting Information Figure S4). The transistor with the 50 wt % IL-doped PS-PIL-PS gate dielectric also did not operate, which indicates that the electrochemical doping of both imidazolium- and pyrrolidinium-type cations affects the performance of n-type organic P(NDI2OD-T2) EGTs. Therefore, we speculate that the electrochemical doping of cations into n-type organic semiconductors plays an important role in device performance. To the best of our knowledge, this kind of study on the influence of electrochemical doping level and dopant type on the device performance in n-type organic EGTs has not been reported. There are no reports for n-type organic EGTs except single crystals[36,37] using either ILs or ion gels as gate dielectrics, which suggests that the unipolar ion conductor is necessary for the operation of n-type organic EGTs. This also supports the speculation about the role of cation doping in the organic semiconductor. However, further studies are needed to elucidate the role of the diffused ions in the organic semiconductor layer and to investigate why the effect of electrochemical doping on the performance of organic EGTs is more serious in n-type EGTs as compared to p-type EGTs.

CONCLUSION

We have demonstrated top-gate n-type organic P(NDI2OD-T2) EGTs by employing a unipolar ion conducting PIL triblock copolymer as the gate insulator. Systematic impedance characterization of PS-PIL-PS at various film thicknesses reveals that there are three polarization regions: (1) dipolar relaxation, (2) ion migration, and (3) EDL formation. These polarization regions shift toward higher frequencies as film thickness is reduced, such that rapid EDL formation can be obtained in thinner polyelectrolyte films despite their lower ion mobility as compared to bipolar electrolytes. Particularly, the 500 nm-thick film shows a favorable capacitance of ~1 μF/cm^2 at 10 kHz. Low voltage operation (<1 V supply) of n-type organic EGTs with unipolar PS-PIL-PS gate insulators was achieved (electron mobility of ~0.008 cm^2/(V·s) and ON/OFF current ratio of ~2 × 10^3). Furthermore, the modulus of this PIL block copolymer is sufficient to allow the subsequent direct deposition of various electrode materials on the polyelectrolytes. By changing gate materials from the high work function PEDOT:PSS to the low work function Al, the threshold voltage (one of the key factors in EGT design) can be tuned from 1 to 0 V in n-type organic EGTs. Electrochemical doping is largely prevented by employing a single ion conducting dielectric, so the formed 2D EDL at the electrolyte/semiconductor interface plays an important role in electrolyte gating of these devices. Because of the attachment of the cations to the backbone of a polymerized ionic liquid, little or no infiltration of ions into an n-type semiconductor is expected. This is consistent with our finding that the 3D electrochemical doping of mobile cations by addition of IL to a unipolar ion conductor diminishes the performance of n-type organic EGTs. This observation appears to be independent of the dopant cation type. Therefore, we speculate that it is necessary to have a unipolar electrolyte to gate n-type organic semiconductors to prevent unfavorable electrochemical doping. Collectively, we anticipate that the use of PIL block copolymer electrolytes as gate insulators will provide unique opportunities to control the extent of electrochemical doping and to select a broader range of gate electrode materials for EGTs, both of which strongly impact the overall device performance. Future work will focus on the fundamental understanding of the role of the infiltrated ions in the organic semiconductor, and the difference in the effect of electrochemical doping on the performance between n-type and p-type organic EGTs. In addition, the use of single ion conductor electrolytes should be explored with other n-type organic EGTs.

EXPERIMENTAL SECTION

Materials. The polymerized ionic liquid triblock copolymer, poly(styrene-*b*-1-[(2-acryloyloxy)ethyl]-3-butylimidazolium bis-(trifluoromethylsulfonyl)imide-*b*-styrene) (denoted as PS-PIL-PS), was synthesized via a two-step sequential reversible addition–fragmentation chain transfer (RAFT) polymerization followed by two postpolymerization reactions, quarternization and anion exchange. The detailed synthetic procedure has been described in a previous report.[42] The molecular weight of the PS-PIL-PS triblock copolymer is 4-252-4 kg/mol. The ionic liquid, 1-ethyl-3-methylimidazolium

DOI: 10.1021/acsami.5b00495
ACS Appl. Mater. Interfaces 2015, 7, 7294–7302

bis(trifluoromethylsulfonyl)imide [EMI][TFSI], was synthesized via an anion exchange reaction.[57] The ionic liquid, 1-butyl-1-methyl pyrrolidinium TFSI, [P14][TFSI], was purchased from Iolitec, Inc. These ionic liquids were dried in a vacuum oven at 70 °C and stored in a glovebox or vacuum desiccator to minimize water contamination. The n-type organic semiconductor, poly{[*N*,*N*′-bis(2-octyldodecyl)-naphthalene-1,4,5,8-bis(dicarboximide)-2,6-diyl]-*alt*-5,5′-(2,2′-bithiophene)} (P(NDI2OD-T2)), was purchased from Polyera Corp.

Preparation of Metal−Insulator−Metal (MIM) Capacitors. 3−7 wt % solutions of PS-PIL-PS triblock copolymer in acetonitrile were prepared and spin-coated (or drop casted) on Au deposited on a SiO_2/Si substrate. An electrolyte film spin-coated at a speed of 2000 rpm for 60 s from a 7 wt % PS-PIL-PS solution typically had a thickness of ∼500 nm. The gold top electrode was thermally evaporated on the electrolyte films using a shadow mask. The detailed experimental setup for the impedance measurements has been described elsewhere.[50] For a 2000 μm-thick film, a homemade cell composed of a Teflon spacer with an inner diameter of 4 mm and a thickness of 2 mm sandwiched between two platinum coated stainless steel electrodes was used. The thicknesses of PS-PIL-PS electrolyte and n-type semiconductor films were measured by a KLA-Tencor P-16 surface profiler.

Device Fabrication. Top-gate bottom-contact thin film transistors were fabricated in ambient conditions except for the vapor deposition of metal electrodes. Source and drain electrodes (5.0 nm Cr/30.0 nm Au) were patterned on SiO_2/Si substrates using photolithography. The channel length and width were 10 and 1000 μm, respectively. A solution of 15 mg/mL P(NDI2OD-T2) n-type semiconductor in dichlorobenzene was spin-coated at 2000 rpm on the substrate, and then annealed at 105 °C for 10 min. Next, the PS-PIL-PS dielectric layer was spin-coated at 2000 rpm from a 7 wt % solution on a semiconductor film. To make bipolar electrolytes, the neat PS-PIL-PS polymer and ionic liquid were codissolved in acetonitrile at a 1:*x*:10 ratio (w/w/w, x = 0.11, 1, and 9). These solutions were spin-coated at 2000 rpm. The dielectric layers were annealed at 105 °C for 1 h. Finally, gate electrodes were fabricated by aerosol jet printing or thermal evaporation. An aqueous PEDOT:PSS ink (PH 500 from H.C. Starck) diluted with 10% (by volume) of ethylene glycol was printed on the electrolyte layer by aerosol jet printing. For metallic gate electrodes, gold, aluminum, and silver gate electrodes were prepared by thermal evaporation with a shadow mask on top of the electrolyte layer.

Characterization. Impedance properties of PS-PIL-PS polyelectrolytes in a metal−insulator−metal (MIM) structure were measured using electrochemical impedance spectroscopy (EIS; Solartron 1255B impedance analyzer, SI 1287 electrochemical interface, ZPlot software). The ZView software was used to fit the experimental impedance data using equivalent circuits. Measurements were conducted over a frequency range of $1-10^6$ Hz with an AC amplitude of 10 mV at room temperature. Current−voltage ($I-V$) characteristics of transistors were measured using Keithley 236 and 6517 electrometers in combination with a Desert Cryogenics (Lakeshore, Inc.) vacuum probe station in a N_2-filled glovebox. All measurements were conducted in a vacuum at a pressure of $<10^{-6}$ Torr.

■ ASSOCIATED CONTENT

Supporting Information

Impedance results for PS−PIL-PS polyelectrolytes as a function of temperature, threshold voltage measurement as a function of work function of the gate material, device characteristics of a P3HT TFT, and device characteristics of n-type organic P(NDI2OD-T2) EGTs with IL([P14][TFSI])-doped PS-PIL-PS polyelectrolyte gate dielectrics. This material is available free of charge via the Internet at http://pubs.acs.org.

■ AUTHOR INFORMATION

Corresponding Authors

*E-mail: frisbie@umn.edu.

*E-mail: lodge@umn.edu.

Notes

The authors declare no competing financial interest.

■ ACKNOWLEDGMENTS

This work was supported by the Air Force Office of Scientific Research (FA9550-12-1-0067). We thank Chang-Hyun Kim for helpful discussions and experimental assistance.

■ REFERENCES

(1) Berggren, M.; Nilsson, D.; Robinson, N. D. Organic Materials for Printed Electronics. *Nat. Mater.* **2007**, *6*, 3−5.

(2) Berggren, M.; Richter-Dahlfors, A. Organic Bioelectronics. *Adv. Mater.* **2007**, *19*, 3201−3213.

(3) Dodabalapur, A. Organic and Polymer Transistors for Electronics. *Mater. Today* **2006**, *9*, 24−30.

(4) Kim, S. H.; Hong, K.; Xie, W.; Lee, K. H.; Zhang, S. P.; Lodge, T. P.; Frisbie, C. D. Electrolyte-Gated Transistors for Organic and Printed Electronics. *Adv. Mater.* **2013**, *25*, 1822−1846.

(5) Braga, D.; Erickson, N. C.; Renn, M. J.; Holmes, R. J.; Frisbie, C. D. High-Transconductance Organic Thin-Film Electrochemical Transistors for Driving Low-Voltage Red-Green-Blue Active Matrix Organic Light-Emitting Devices. *Adv. Funct. Mater.* **2012**, *22*, 1623−1631.

(6) Andersson, P.; Forchheimer, R.; Tehrani, P.; Berggren, M. Printable All-Organic Electrochromic Active-Matrix Displays. *Adv. Funct. Mater.* **2007**, *17*, 3074−3082.

(7) Lin, P.; Yan, F. Organic Thin-Film Transistors for Chemical and Biological Sensing. *Adv. Mater.* **2012**, *24*, 34−51.

(8) Xia, Y.; Zhang, W.; Ha, M. J.; Cho, J. H.; Renn, M. J.; Kim, C. H.; Frisbie, C. D. Printed Sub-2 V Gel-Electrolyte-Gated Polymer Transistors and Circuits. *Adv. Funct. Mater.* **2010**, *20*, 587−594.

(9) Herlogsson, L.; Colle, M.; Tierney, S.; Crispin, X.; Berggren, M. Low-Voltage Ring Oscillators Based on Polyelectrolyte-Gated Polymer Thin-Film Transistors. *Adv. Mater.* **2010**, *22*, 72−76.

(10) Zhao, J.; Shen, X. J.; Yan, F.; Qiu, L. H.; Lee, S. T.; Sun, B. Q. Solvent-Free Ionic Liquid/Poly(ionic liquid) Electrolytes for Quasi-Solid-State Dye-Sensitized Solar Cells. *J. Mater. Chem.* **2011**, *21*, 7326−7330.

(11) Kim, T.; Kirn, H.; Kwon, S. W.; Kim, Y.; Park, W. K.; Yoon, D. H.; Jang, A. R.; Shin, H. S.; Suh, K. S.; Yang, W. S. Large-Scale Graphene Micropatterns via Self-Assembly-Mediated Process for Flexible Device Application. *Nano Lett.* **2012**, *12*, 743−748.

(12) Kim, B. J.; Lee, S. K.; Kang, M. S.; Ahn, J. H.; Cho, J. H. Coplanar-Gate Transparent Graphene Transistors and Inverters on Plastic. *ACS Nano* **2012**, *6*, 8646−8651.

(13) Larsson, O.; Said, E.; Berggren, M.; Crispin, X. Insulator Polarization Mechanisms in Polyelectrolyte-Gated Organic Field-Effect Transistors. *Adv. Funct. Mater.* **2009**, *19*, 3334−3341.

(14) Herlogsson, L.; Crispin, X.; Robinson, N. D.; Sandberg, M.; Hagel, O. J.; Gustafsson, G.; Berggren, M. Low-Voltage Polymer Field-Effect Transistors Gated via a Proton Conductor. *Adv. Mater.* **2007**, *19*, 97−101.

(15) Cho, J. H.; Lee, J.; Xia, Y.; Kim, B.; He, Y. Y.; Renn, M. J.; Lodge, T. P.; Frisbie, C. D. Printable Ion-Gel Gate Dielectrics for Low-Voltage Polymer Thin-Film Transistors on Plastic. *Nat. Mater.* **2008**, *7*, 900−906.

(16) Lee, J.; Kaake, L. G.; Cho, J. H.; Zhu, X. Y.; Lodge, T. P.; Frisbie, C. D. Ion Gel-Gated Polymer Thin-Film Transistors: Operating Mechanism and Characterization of Gate Dielectric Capacitance, Switching Speed, and Stability. *J. Phys. Chem. C* **2009**, *113*, 8972−8981.

(17) Herlogsson, L.; Noh, Y. Y.; Zhao, N.; Crispin, X.; Sirringhaus, H.; Berggren, M. Downscaling of Organic Field-Effect Transistors with a Polyelectrolyte Gate Insulator. *Adv. Mater.* **2008**, *20*, 4708−4713.

(18) Yomogida, Y.; Pu, J.; Shimotani, H.; Ono, S.; Hotta, S.; Iwasa, Y.; Takenobu, T. Ambipolar Organic Single-Crystal Transistors Based on Ion Gels. *Adv. Mater.* **2012**, *24*, 4392−4397.

DOI: 10.1021/acsami.5b00495
ACS Appl. Mater. Interfaces 2015, 7, 7294−7302

(19) Panzer, M. J.; Newman, C. R.; Frisbie, C. D. Low-Voltage Operation of a Pentacene Field-Effect Transistor with a Polymer Electrolyte Gate Dielectric. *Appl. Phys. Lett.* **2005**, *86*, 103503.
(20) Xie, W.; Frisbie, C. D. Organic Electrical Double Layer Transistors Based on Rubrene Single Crystals: Examining Transport at High Surface Charge Densities above 10^{13} cm^{-2}. *J. Phys. Chem. C* **2011**, *115*, 14360−14368.
(21) Zhang, Y. J.; Ye, J. T.; Matsuhashi, Y.; Iwasa, Y. Ambipolar MoS_2 Thin Flake Transistors. *Nano Lett.* **2012**, *12*, 1136−1140.
(22) Thiemann, S.; Sachnov, S. J.; Pettersson, F.; Bollstrom, R.; Osterbacka, R.; Wasserscheid, P.; Zaumseil, J. Cellulose-Based Ionogels for Paper Electronics. *Adv. Funct. Mater.* **2014**, *24*, 625−634.
(23) Yamada, Y.; Ueno, K.; Fukumura, T.; Yuan, H. T.; Shimotani, H.; Iwasa, Y.; Gu, L.; Tsukimoto, S.; Ikuhara, Y.; Kawasaki, M. Electrically Induced Ferromagnetism at Room Temperature in Cobalt-Doped Titanium Dioxide. *Science* **2011**, *332*, 1065−1067.
(24) Kang, M. S.; Lee, J.; Norris, D. J.; Frisbie, C. D. High Carrier Densities Achieved at Low Voltages in Ambipolar PbSe Nanocrystal Thin-Film Transistors. *Nano Lett.* **2009**, *9*, 3848−3852.
(25) Park, S. Y.; Kim, B. J.; Kim, K.; Kang, M. S.; Lim, K. H.; Il Lee, T.; Myoung, J. M.; Baik, H. K.; Cho, J. H.; Kim, Y. S. Low-Temperature, Solution-Processed and Alkali Metal Doped ZnO for High-Performance Thin-Film Transistors. *Adv. Mater.* **2012**, *24*, 834−838.
(26) Bubel, S.; Meyer, S.; Kunze, F.; Chabinyc, M. L. Ionic Liquid Gating Reveals Trap-Filled Limit Mobility in Low Temperature Amorphous Zinc Oxide. *Appl. Phys. Lett.* **2013**, *103*, 152102.
(27) Xie, W.; Frisbie, C. D. Electrolyte Gated Single-Crystal Organic Transistors to Examine Transport in the High Carrier Density Regime. *MRS Bull.* **2013**, *38*, 43−50.
(28) Shimotani, H.; Diguet, G.; Iwasa, Y. Direct Comparison of Field-Effect and Electrochemical Doping in Regioregular Poly(3-hexylthiophene). *Appl. Phys. Lett.* **2005**, *86*, 022104.
(29) Yuan, H.; Shimotani, H.; Tsukazaki, A.; Ohtomo, A.; Kawasaki, M.; Iwasa, Y. High-Density Accumulation in ZnO Field-Effect Transistors Gated by Electric Double Layers of Ionic Liquids. *Adv. Funct. Mater.* **2009**, *19*, 1046−1053.
(30) Panzer, M. J.; Frisbie, C. D. Polymer Electrolyte-Gated Organic Field-Effect Transistors: Low-Voltage, High-Current Switches for Organic Electronics and Testbeds for Probing Electrical Transport at High Charge Carrier Density. *J. Am. Chem. Soc.* **2007**, *129*, 6599−6607.
(31) Panzer, M. J.; Frisbie, C. D. High Carrier Density and Metallic Conductivity in Poly(3-hexylthiophene) Achieved by Electrostatic Charge Injection. *Adv. Funct. Mater.* **2006**, *16*, 1051−1056.
(32) Fabiano, S.; Braun, S.; Fahlman, M.; Crispin, X.; Berggren, M. Effect of Gate Electrode Work-Function on Source Charge Injection in Electrolyte-Gated Organic Field-Effect Transistors. *Adv. Funct. Mater.* **2014**, *24*, 695−700.
(33) Laiho, A.; Nguyen, H. T.; Sinno, H.; Engquist, I.; Berggren, M.; Dubois, P.; Coulembier, O.; Crispin, X. Amphiphilic Poly(3-hexylthiophene)-Based Semiconducting Copolymers for Printing of Polyelectrolyte-Gated Organic Field-Effect Transistors. *Macromolecules* **2013**, *46*, 4548−4557.
(34) Laiho, A.; Herlogsson, L.; Forchheimer, R.; Crispin, X.; Berggren, M. Controlling the Dimensionality of Charge Transport in Organic Thin-Film Transistors. *Proc. Natl. Acad. Sci. U.S.A.* **2011**, *108*, 15069−15073.
(35) Panzer, M. J.; Frisbie, C. D. Polymer Electrolyte Gate Dielectric Reveals Finite Windows of High Conductivity in Organic Thin Film Transistors at High Charge Carrier Densities. *J. Am. Chem. Soc.* **2005**, *127*, 6960−6961.
(36) Ono, S.; Minder, N.; Chen, Z.; Facchetti, A.; Morpurgo, A. F. High-Performance N-type Organic Field-Effect Transistors with Ionic Liquid Gates. *Appl. Phys. Lett.* **2010**, *97*, 143307.
(37) Uemura, T.; Yamagishi, M.; Ono, S.; Takeya, J. Low-Voltage Operation of N-type Organic Field-Effect Transistors with Ionic Liquid. *Appl. Phys. Lett.* **2009**, *95*, 103301.
(38) Malti, A.; Gabrielsson, E. O.; Berggren, M.; Crispin, X. Ultra-Low Voltage Air-Stable Polyelectrolyte Gated N-type Organic Thin Film Transistors. *Appl. Phys. Lett.* **2011**, *99*, 063305.
(39) Herlogsson, L.; Crispin, X.; Tierney, S.; Berggren, M. Polyelectrolyte-Gated Organic Complementary Circuits Operating at Low Power and Voltage. *Adv. Mater.* **2011**, *23*, 4684−4689.
(40) Ye, Y. S.; Sharick, S.; Davis, E. M.; Winey, K. I.; Elabd, Y. A. High Hydroxide Conductivity in Polymerized Ionic Liquid Block Copolymers. *ACS Macro Lett.* **2013**, *2*, 575−580.
(41) Choi, J. H.; Ye, Y. S.; Elabd, Y. A.; Winey, K. I. Network Structure and Strong Microphase Separation for High Ion Conductivity in Polymerized Ionic Liquid Block Copolymers. *Macromolecules* **2013**, *46*, 5290−5300.
(42) Gu, Y. Y.; Lodge, T. P. Synthesis and Gas Separation Performance of Triblock Copolymer Ion Gels with a Polymerized Ionic Liquid Mid-Block. *Macromolecules* **2011**, *44*, 1732−1736.
(43) Yuan, J. Y.; Antonietti, M. Poly(ionic liquid)s: Polymers Expanding Classical Property Profiles. *Polymer* **2011**, *52*, 1469−1482.
(44) Yuan, J. Y.; Mecerreyes, D.; Antonietti, M. Poly(ionic liquid)s: An Update. *Prog. Polym. Sci.* **2013**, *38*, 1009−1036.
(45) Lee, M.; Choi, U. H.; Salas-de la Cruz, D.; Mittal, A.; Winey, K. I.; Colby, R. H.; Gibson, H. W. Imidazolium Polyesters: Structure-Property Relationships in Thermal Behavior, Ionic Conductivity, and Morphology. *Adv. Funct. Mater.* **2011**, *21*, 708−717.
(46) Ye, Y. S.; Elabd, Y. A. Anion Exchanged Polymerized Ionic Liquids: High Free Volume Single Ion Conductors. *Polymer* **2011**, *52*, 1309−1317.
(47) Horowitz, A. I.; Panzer, M. J. High-Performance, Mechanically Compliant Silica-based Ionogels for Electrical Energy Storage Applications. *J. Mater. Chem.* **2012**, *22*, 16534−16539.
(48) Marcilla, R.; Alcaide, F.; Sardon, H.; Pomposo, J. A.; Pozo-Gonzalo, C.; Mecerreyes, D. Tailor-made Polymer Electrolytes based upon Ionic Liquids and Their Application in All-plastic Electrochromic devices. *Electrochem. Commun.* **2006**, *8*, 482−488.
(49) Zhang, S. P.; Lee, K. H.; Frisbie, C. D.; Lodge, T. P. Ionic Conductivity, Capacitance, and Viscoelastic Properties of Block Copolymer-Based Ion Gels. *Macromolecules* **2011**, *44*, 940−949.
(50) Lee, K. H.; Zhang, S. P.; Lodge, T. P.; Frisbie, C. D. Electrical Impedance of Spin-Coatable Ion Gel Films. *J. Phys. Chem. B* **2011**, *115*, 3315−3321.
(51) Brug, G. J.; Vandeneeden, A. L. G.; Sluytersrehbach, M.; Sluyters, J. H. The Analysis of Electrode Impedances Complicated by the Presence of a Constant Phase Element. *J. Electroanal. Chem.* **1984**, *176*, 275−295.
(52) Pajkossy, T. Impedance of Rough Capacitive Electrodes. *J. Electroanal. Chem.* **1994**, *364*, 111−125.
(53) Lee, K. H.; Kang, M. S.; Zhang, S. P.; Gu, Y. Y.; Lodge, T. P.; Frisbie, C. D. "Cut and Stick" Rubbery Ion Gels as High Capacitance Gate Dielectrics. *Adv. Mater.* **2012**, *24*, 4457−4462.
(54) Yan, H.; Chen, Z. H.; Zheng, Y.; Newman, C.; Quinn, J. R.; Dotz, F.; Kastler, M.; Facchetti, A. A High-Mobility Electron-Transporting Polymer for Printed Transistors. *Nature* **2009**, *457*, 679−687.
(55) Kergoat, L.; Herlogsson, L.; Piro, B.; Pham, M. C.; Horowitz, G.; Crispin, X.; Berggren, M. Tuning the Threshold Voltage in Electrolyte-Gated Organic Field-Effect Transistors. *Proc. Natl. Acad. Sci. U.S.A.* **2012**, *109*, 8394−8399.
(56) Kaake, L. G.; Zou, Y.; Panzer, M. J.; Frisbie, C. D.; Zhu, X. Y. Vibrational Spectroscopy Reveals Electrostatic and Electrochemical Doping in Organic Thin Film Transistors Gated with a Polymer Electrolyte Dielectric. *J. Am. Chem. Soc.* **2007**, *129*, 7824−7830.
(57) Susan, M. A.; Kaneko, T.; Noda, A.; Watanabe, M. Ion Gels Prepared by in Situ Radical Polymerization of Vinyl Monomers in an Ionic Liquid and Their Characterization as Polymer Electrolytes. *J. Am. Chem. Soc.* **2005**, *127*, 4976−4983.

DOI: 10.1021/acsami.5b00495
ACS Appl. Mater. Interfaces 2015, 7, 7294−7302